Chapter 1

Body MR imaging at 3T: basic considerations about artifacts and safety

Kevin J. Chang and Ihab R. Kamel

Introduction

Three Tesla magnetic resonance (MR) imaging scanners have been seeing steadily increasing use recently as hardware has matured and pulse sequences have become more optimized for a higher field strength. This increase in popularity has been more pronounced for neurologic and musculoskeletal imaging than for body imaging, however, due to the fact that 3T imaging with the larger field of view required for the torso tends to be more susceptible to artifacts and energy absorption limits than the imaging of smaller body parts.

Imaging artifacts at 3T tend to be more numerous and/or more pronounced than at lower field strengths [1]. While most of these artifacts are the same ones encountered at lower field strengths (e.g., flow artifacts, motion artifacts, Gibbs ringing), many are more peculiar to high-field imaging. This chapter will discuss these field strength-related artifacts at 3T as they apply to body imaging with specific comparisons made to 1.5T. The differences in relaxation times, chemical shift effects, and issues related to field inhomogeneity will also be discussed. Various approaches to mitigating artifacts peculiar to an increase in field strength at 3T will also be addressed.

Signal-to-noise ratio

MR signal relates directly to the ratio of protons aligned parallel rather than anti-parallel to the static magnetic field (B0). This ratio varies by the square of the magnetic field strength so a doubling of field strength from 1.5T to 3T should result in a quadrupling of MR signal. However, the doubling of field strength is also accompanied by a doubling of noise. The net effect of these changes results in an overall theoretical doubling of the signal-to-noise ratio (SNR). Thus, the theoretical SNR varies directly with the increase in magnetic field strength. It is this promised gain in SNR from an increase in field strength that allows for a boost in spatial resolution, temporal resolution, or some combination of the two. An increase in SNR also promises to improve MR spectroscopy and diffusion-weighted imaging. In practice, however, moving from 1.5T to 3T usually results in a less than twofold realized gain in SNR due to physiologic noise and limitations in energy deposition as well as other factors such as inadequate optimization of scanner hardware and software, radiofrequency (RF) field (B1) inhomogeneity, and increased magnetic susceptibility effects.

T1 relaxation times

For most physiologic tissues an increase in magnetic field strength leads to a prolongation of T1 relaxation times [2]. When attempting to generate soft tissue contrast at 3T, a longer repetition time (TR) may be required to obtain a similar imaging appearance that one may be accustomed to at 1.5T and lower field strengths (Figures 1.1 and 1.2) [3]. The downside of a longer TR is a concomitant increase in imaging time. T1 relaxation times tend to be approximately 20–40% longer at 3T when compared with 1.5T [2].

Approaches to addressing this problem with unenhanced T1-weighted images include the addition of an inversion recovery preparatory pulse to accentuate T1 contrast (e.g., T1 fluid-attenuated inversion recovery [FLAIR]). Other possibilities include the use of magnetization preparation pulses, short echo time (TE) gradient echo pulses, as well as parallel imaging techniques to decrease overall imaging time [4, 5].

Body MR Imaging at 3 Tesla, ed. Ihab R. Kamel and Elmar M. Merkle. Published by Cambridge University Press.

Gadolinium contrast effects

While the T1 relaxation time of unenhanced soft tissues is longer at 3T compared with lower field strengths, the T1 relaxation time of gadolinium chelate-based contrast agents is relatively unaffected. As a result, post-contrast imaging at 3T yields a more conspicuous degree of contrast enhancement. This wider dynamic range of effect leads to an increase in the contrast-to-noise ratio (CNR), an effect illustrated in Figures 1.3 and 1.4.

An increase in CNR at 3T leads to increased target conspicuity on post-contrast imaging, improved vessel delineation and visualization on MR angiography (MRA), as well as the possibility of decreasing contrast dose compared with 1.5T [6–8] This latter option is becoming increasingly relevant due to the heightened awareness of the risks of nephrogenic systemic fibrosis (NSF). In fact, for imaging of brain tumors, a half dose of gadolinium-based contrast at 3T approximates the CNR of a full dose of contrast at 1.5T [8].

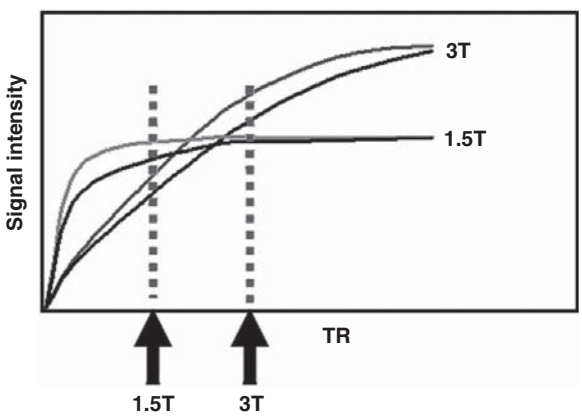

Figure 1.1 Signal intensity–time curves show longer T1 relaxation times at MR imaging in liver (black curves) and tumor tissue (gray curves) at 3T than at 1.5T. To generate a level of T1 contrast between the two tissue types at 3T commensurate with that at 1.5T, longer repetition times (TR, represented by dotted vertical lines) are required. Reproduced with permission from Chang KJ, Kamel IR, Macura KJ, Bluemke DA. 3T MR imaging of the abdomen: comparison with 1.5T. *RadioGraphics* 2008; **28**: 1983–98. © Radiological Society of North America.

T2 and T2* relaxation times (magnetic susceptibility)

The effects of an increase in field strength on the T2 relaxation times of tissues are less predictable than the changes in T1 relaxation times. While for lattice-fixed protons, T2 relaxation times may be similarly prolonged with an increase in field strength, most tissues experience an increase in efficiency of chemical exchange mechanisms at 3T which tends to result in a net shortening of T2 relaxation times (the efficiency of proton exchange between molecules varies with the square of the magnetic field strength). While for most soft tissues, T2 relaxation times are slightly shorter, T2 relaxation times for adipose tissues remain slightly

(a)

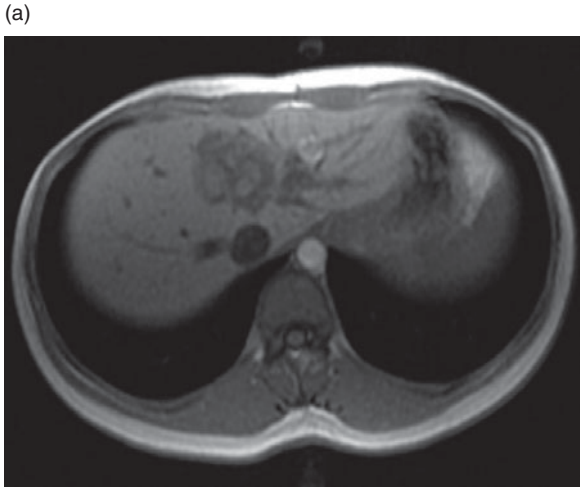

(b)

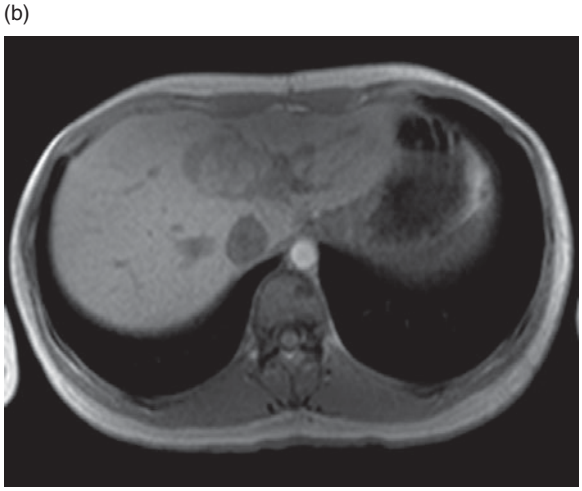

Figure 1.2 Effect of higher magnetic field strength on the visibility of a colon adenocarcinoma metastasis in the liver of a 32-year-old woman. Unenhanced T1-weighted gradient echo images obtained at 1.5T with 180/4.4 (TR ms/echo time [TE] ms), 90° flip angle, and 8-mm section thickness (a) and at 3T with 263/2.3, 75° flip angle, and 8-mm section thickness (b) show higher SNR but decreased lesion conspicuity in (b).

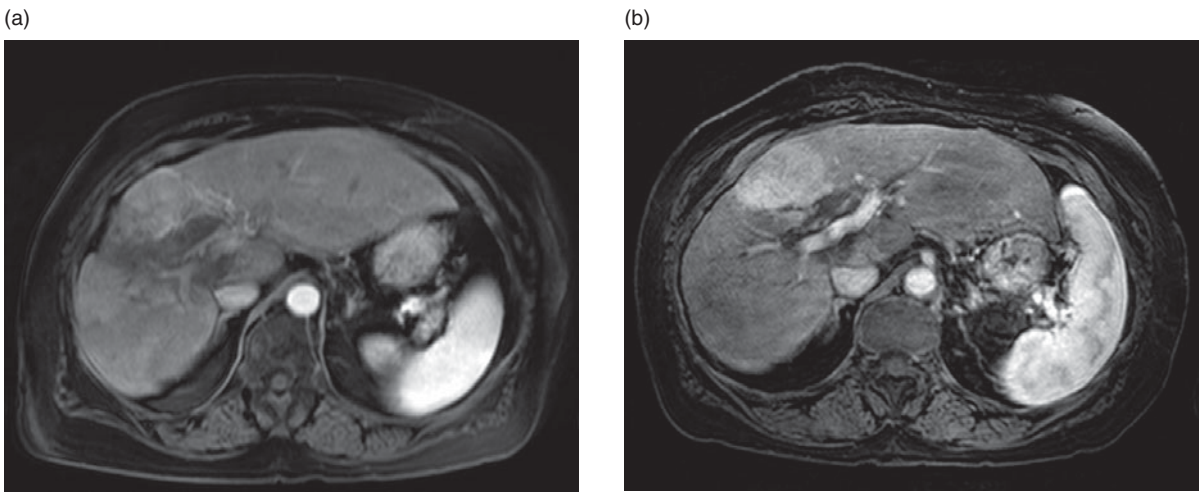

Figure 1.3 Increased conspicuity of lesions at 3T MR. Gadolinium-induced contrast enhancement of a moderately differentiated cholangiocarcinoma in an 82-year-old woman is less pronounced on the 1.5T three-dimensional (3D) volumetric interpolated breath-hold examination (VIBE; 4.9/2.5, 10° flip angle) image (a) than on the 3T 3D T1-weighted high-resolution isotropic volume examination (THRIVE; 3.3/1.6, 10° flip angle) image (b) because of lower CNR at 1.5T compared with 3T, even allowing for equipment differences.

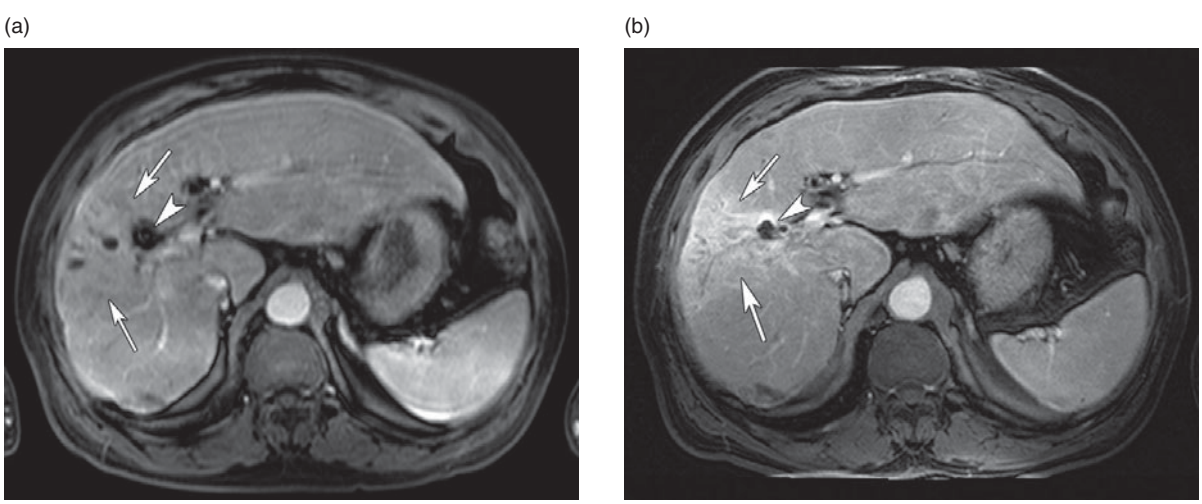

Figure 1.4 Increased conspicuity of lesions at 3T MR. Comparison of 1.5T 3D VIBE (4.9/2.5, 10° flip angle) (a) and 3T 3D THRIVE (3.3/1.6, 10° flip angle) (b) MR images in a 68-year-old man with hepatitis C-related cirrhosis shows greater contrast of a wedge-shaped region of hyperperfusion (transient hepatic signal intensity difference) (arrows) at 3T than at 1.5T. Magnetic susceptibility artifacts related to a surgical clip (arrowheads) also are partially mitigated in (b) because of the use of a shorter TE.

longer and T2 relaxation times for fluids are largely unchanged [2].

Nevertheless, there is a significant perceived improvement in image quality on T2-weighted images with a move to a higher field strength (Figure 1.5). This is chiefly related to an increase in SNR and is more pronounced on T2-weighted imaging than T1-weighted imaging as the longer TR of T2-weighted pulse sequences allows for more recovery of longitudinal magnetization than on T1-weighted sequences. Sequences such as single-shot fast spin echo (SSFSE), half-Fourier acquisition single-shot turbo spin echo (HASTE), as well as three-dimensional (3D) turbo spin echo (such as in 3D MR cholangiopancreatography) stand to benefit the most from a higher field strength.

T2* relaxation times are affected much more predictably with a move to 3T and vary inversely

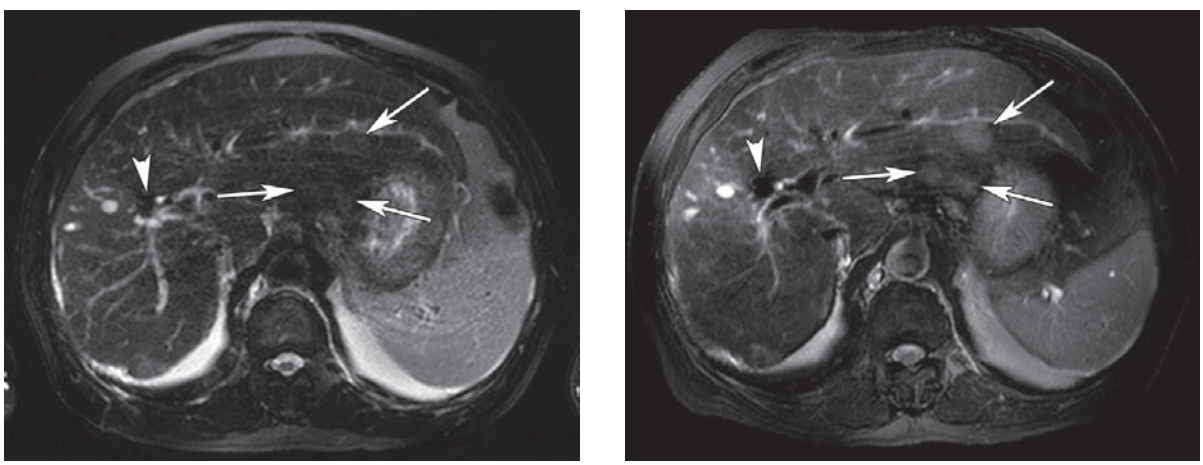

Figure 1.5 T2-weighted fast spin echo images in a 68-year-old male with hepatocellular carcinoma in the setting of hepatitis C-associated cirrhosis (same patient as Figure 1.4 but at a slightly different level) at 1.5T (a) and 3T (b). Multiple T2-intense metastases (white arrows) are more apparent at 3T than 1.5T (3T examination 1 month prior to 1.5T examination). Also note the increased susceptibility related to a metallic clip (white arrowhead) in the central right lobe at 3T which is barely perceptible at 1.5T. Parameters: (a) 1.5T 4000/103/90°. (b) 3T 2053/100/90°.

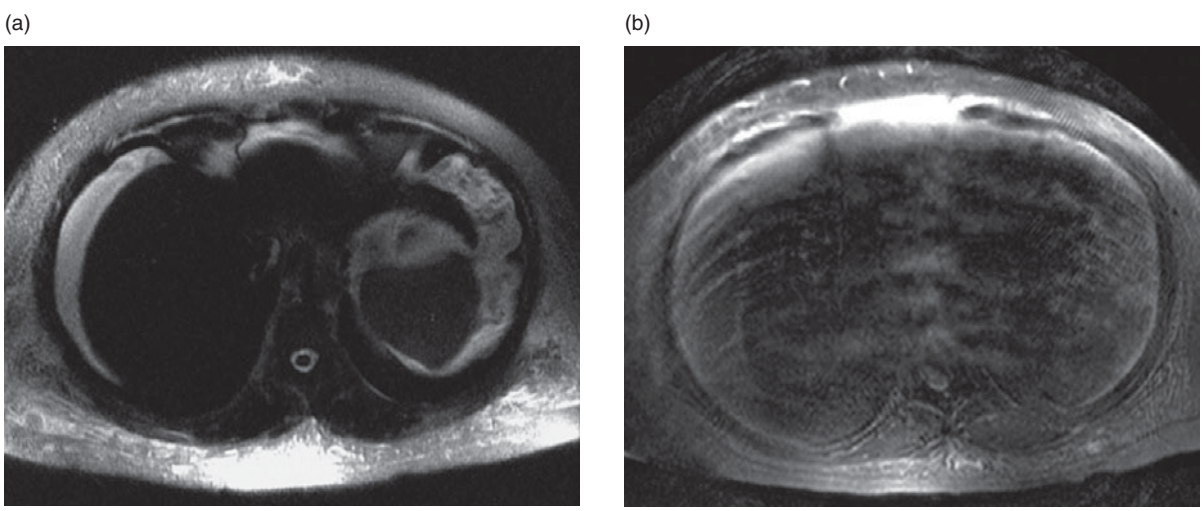

Figure 1.6 Field inhomogeneity and standing wave effects. T2-weighted images through the liver at 1.5T (2416/180) (a) and at 3T (2052/100) (b) show diffuse hepatic iron deposition and ascites in a 49-year-old woman with hepatitis C–related cirrhosis. In (b), there is increased susceptibility artifact and decreased signal intensity in the liver because of iron deposition, standing wave effects with signal drop-off related to ascites (seen in the central abdomen), and significant respiratory motion artifact. Reproduced with permission from Chang KJ, Kamel IR, Macura KJ, Bluemke DA. 3T MR imaging of the abdomen: comparison with 1.5T. *RadioGraphics* 2008; **28**: 1983–98.

with the strength of the magnetic field [9, 10]. Thus, a doubling of field strength from 1.5T to 3T results in a doubling of magnetic susceptibility artifact and a larger area of "blooming" related to paramagnetic effects. This has a particularly profound effect on gradient echo images and echo planar pulse sequences such as those commonly used in diffusion-weighted imaging and functional MR imaging. When used in conventional imaging, the more pronounced magnetic susceptibility at air–soft tissue interfaces and areas adjacent to paramagnetic materials such as metals can lead to significant localized variations in magnetic field homogeneity (inhomogeneous B0 field, Figure 1.6). This results in larger artifactual signal voids than at 1.5T. This effect does, however, allow for higher sensitivity to

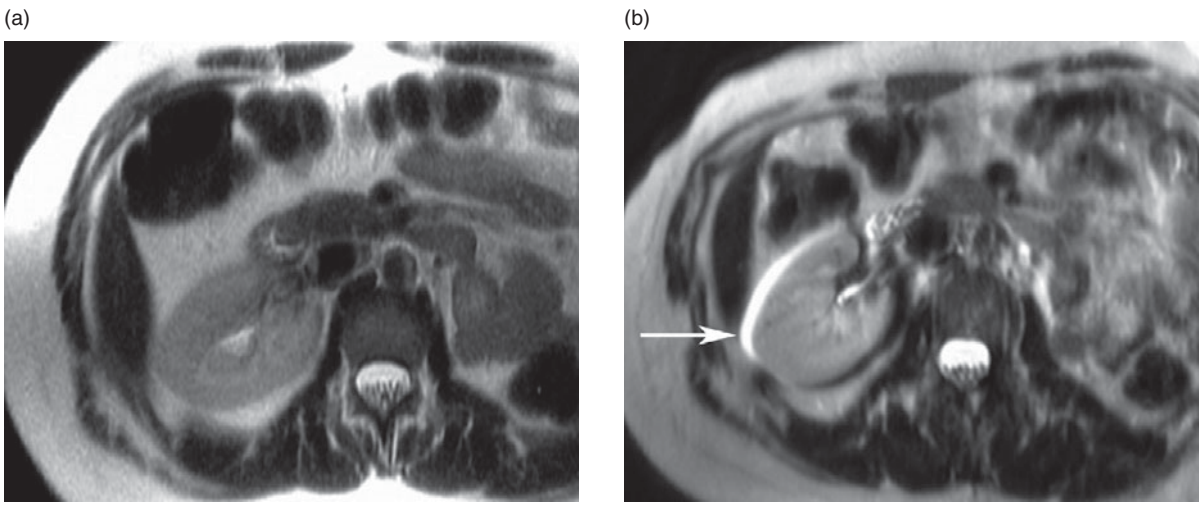

Figure 1.7 Chemical shift artifact at 1.5T (a) and 3T (b) in normal kidneys. Note increased water–fat misregistration at the renal cortex at 3T (white arrow). Parameters: (a) 1.5T SSFSE 1759/88, slice thickness 8 mm. (b) 3T SSFSE 4500/90, slice thickness 8 mm. Reproduced with permission from Chang KJ, Kamel IR, Macura KJ, Bluemke DA. 3T MR imaging of the abdomen: comparison with 1.5T. *RadioGraphics* 2008; **28**: 1983–98. © Radiological Society of North America.

the detection of gas, items such as surgical clips, and areas of iron deposition in solid organs. This effect, in fact, makes 3T imaging more sensitive to superparamagnetic iron oxide contrast agents (SPIO) as well as the blood oxygen level-dependent (BOLD) phenomenon used extensively in functional MR imaging [11–13].

Approaches to minimizing magnetic susceptibility artifacts include shortening TE, using parallel imaging to shorten imaging time and decrease echo train length, and increasing receiver bandwidth to decrease the echo spacing of the readout train. These approaches have already shown significant success in reducing artifacts on diffusion-weighted imaging in the brain [14, 15].

Chemical shift effects

Just as with magnetic susceptibility effects, chemical shift effects also directly vary with an increase in the magnetic field strength. For chemical shift effects of the first kind, the difference in precession frequency of water protons and fat protons holds steady at 3.5 ppm. With a doubling of field strength from 1.5T to 3T the Larmor frequency doubles from 64 MHz to 128 MHz, respectively. Accompanying this doubling of Larmor frequency is a chemical shift separation between water and fat which also doubles from approximately 220 Hz to 440 Hz, respectively (Larmor frequency × 3.5 ppm). This means at a constant bandwidth, the misregistration artifacts between fat voxels and water voxels in the frequency-encoding direction doubles in conspicuity with a doubling in field strength (Figure 1.7). While this misregistration artifact is more pronounced at 3T, this wider spectral separation between fat and water also allows for improved spectral resolution in MR spectroscopy as well as improved fat suppression limited only by the degree of magnetic field inhomogeneity [16, 17].

There are various approaches to decreasing the conspicuity of the misregistration artifact associated with chemical shift effects of the first kind. An increase in bandwidth will counteract an increase in chemical shift at the cost of SNR. For example, a doubling of bandwidth to fully offset a doubling of field strength will result in a 29% decrease in relative SNR. This ability to increase bandwidth is limited by gradient coil strength. Another approach to mitigating fat–water misregistration is utilizing fat suppression.

Chemical shift artifacts of the second kind are also significantly affected by an increase in magnetic field strength. These phase cancellation or "India ink" artifacts are seen in voxels sharing both fat and water protons at specific TEs corresponding to times when fat and water protons precess out of phase with each other resulting in signal cancellation. This is most commonly seen at the edges of solid organs where

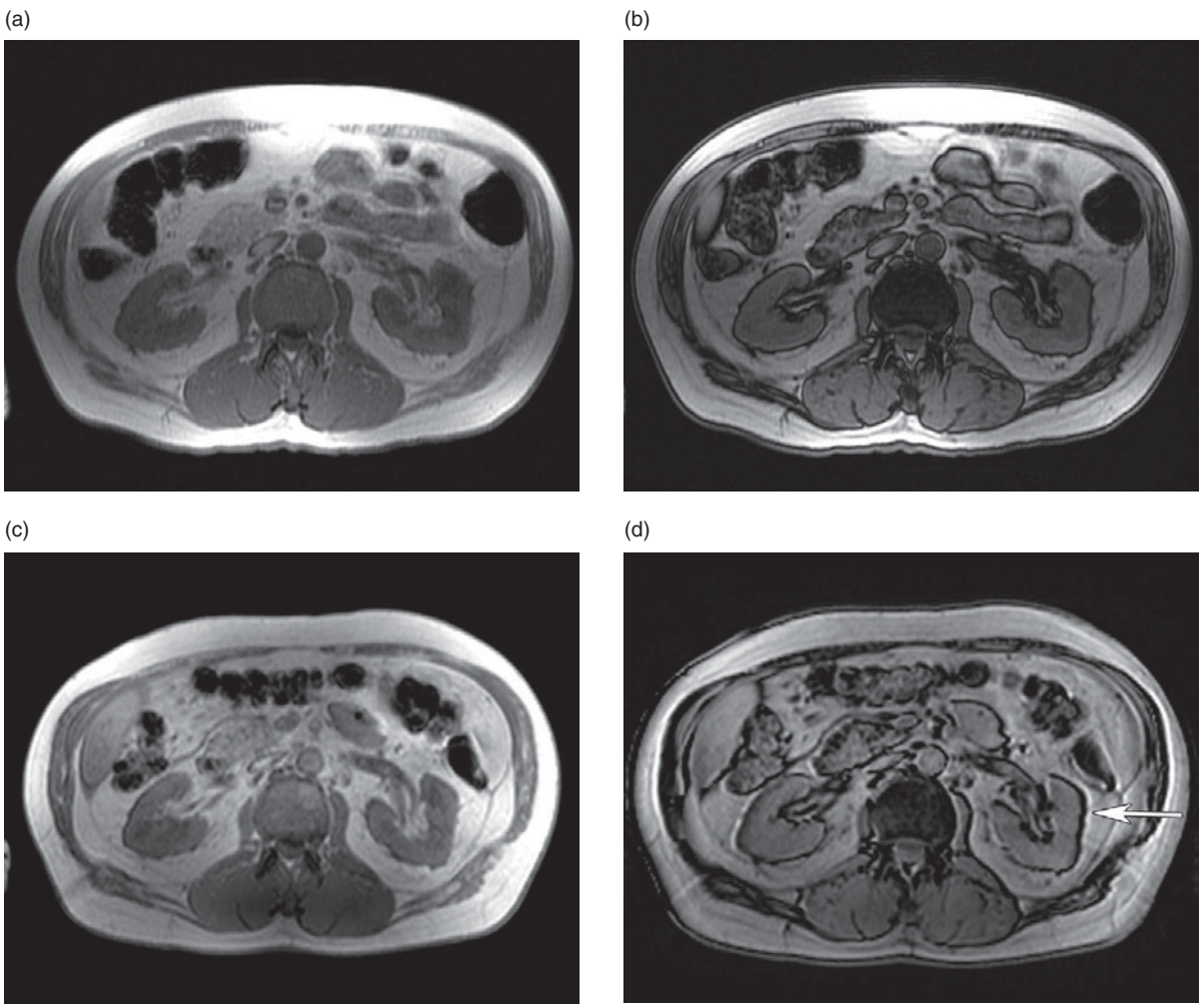

Figure 1.8 In-phase and out-of-phase imaging at 1.5T and 3T. (a) 1.5T in-phase TE 4.6 ms. (b) 1.5T out-of-phase TE 2.3 ms. (c) 3T in-phase TE 2.3 ms. (d) 3T out-of-phase TE 1.15 ms. Note increased chemical shift at 3T (white arrow).

they interface with surrounding fat. A doubling of field strength will double the precession frequency of these protons and, correspondingly, halve their out-of-phase and in-phase TEs from approximately 2.3 and 4.6 ms respectively at 1.5T to approximately 1.15 and 2.3 ms at 3T (Figure 1.8) [18]. When gradient coils are incapable of imaging with a TE as short as 1.15 ms, significant changes may need to be incorporated when obtaining T1-weighted in- and out-of-phase images routine in abdominal imaging. If the next shortest out-of-phase TE of 3.45 ms is obtained, if compared with an in-phase image at TE 2.3 ms, magnetic susceptibility effects related to a longer TE cannot be differentiated from signal dropout related to chemical shift effects of the second kind. An alternative approach is obtaining two separate image acquisitions rather than using a dual-echo pulse sequence; however, this introduces problems related to imperfect image co-registration of the two acquisitions and necessitates longer imaging time. Another approach is the use of a dual-echo 3D fast spoiled gradient echo pulse sequence [19].

Field inhomogeneity (B0, B1, and dielectric shading)

One of the most apparent challenges faced with MR imaging at 3T relates to significant variations in signal intensity that are often encountered across the field of

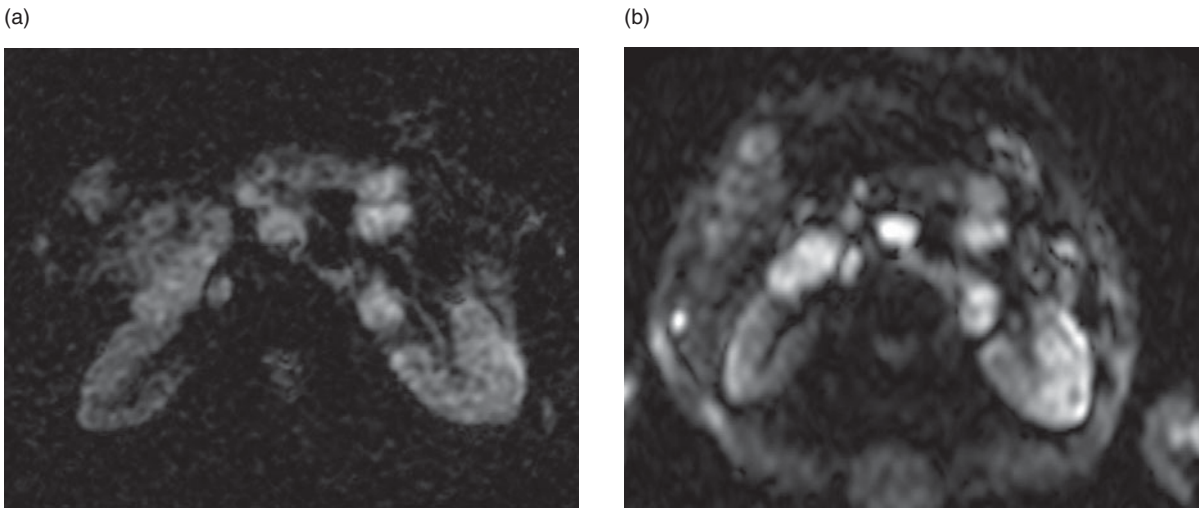

Figure 1.9 Diffusion-weighted imaging of normal kidneys in the axial plane at 1.5T (a) and 3T (b), B = 750 s/mm^2. Higher SNR at 3T increases sensitivity for areas of restricted diffusion. Image quality may be limited by increased sensitivity to magnetic susceptibility artifact. Reproduced with permission from Chang KJ, Kamel IR, Macura KJ, Bluemke DA. 3T MR imaging of the abdomen: comparison with 1.5T. *RadioGraphics* 2008; **28**: 1983–98. © Radiological Society of North America.

view, especially with the larger field of view required in imaging the human torso. Multiple factors can account for these signal intensity variations across an image. As has been discussed above, increased sensitivity to T2* effects can lead to pronounced magnetic susceptibility effects, especially in areas adjacent to air or the skin surface. This effect is commonly seen in the upper abdomen adjacent to the lung bases as well as around gas-filled loops of bowel. Gradient echo and echo planar acquisitions such as those typically used in diffusion-weighted imaging can be quite susceptible to these effects (Figure 1.9), although, when combined with the use of parallel imaging, diffusion-weighted imaging at 3T can be performed more quickly and with higher SNR [15]. In addition, underlying B0 field inhomogeneities have been a challenge addressed with some success on newer-generation 3T scanners, with improvements in B0 field homogeneity through better shimming and magnet design. Other approaches to limiting B0 field inhomogeneity are similar to limiting susceptibility artifact and include shortening TE (which may require an increase in bandwidth and resultant decrease in SNR), using parallel imaging to shorten imaging time, and decreasing voxel size to limit intravoxel dephasing.

Another major factor accounting for signal intensity variations on 3T images is inhomogeneity in the B1 or RF field. Particularly with larger fields of view such as in the abdomen and pelvis, standing wave or dielectric effects become a significant source of RF field inhomogeneity at 3T. The reason why these effects are so much more pronounced at 3T than at lower field strengths is related to the RF wavelength corresponding to the resonant frequency (Larmor frequency) of water protons. While at 1.5T a Larmor frequency of 64 MHz corresponds to an RF wavelength of 52 cm, at 3T a higher Larmor frequency of 128 MHz corresponds to a shorter wavelength of 26 cm, which is much closer in dimension to the human abdomen or pelvis. These wavelengths lead to areas of constructive and destructive interference within the torso, termed standing wave or "dielectric shading" effects, which can lead to large variations in local signal intensity across an image [20]. This finding is more apparent in those with a wider body habitus or more ellipsoid body cross section [21]. Similar-appearing artifacts can be even more troublesome in patients with a large volume of conductive intra-abdominal fluid such as ascites or amniotic fluid. Rapid alterations in the magnetic field caused by changing RF currents tend to induce circulating currents within large volumes of conductive fluid that counteract or "shield" the RF field and attenuate signal intensity within the central torso (Figure 1.10) [22]. This "black-hole" artifact tends to be more noticeable with fast spin echo pulse sequences than gradient echo sequences.

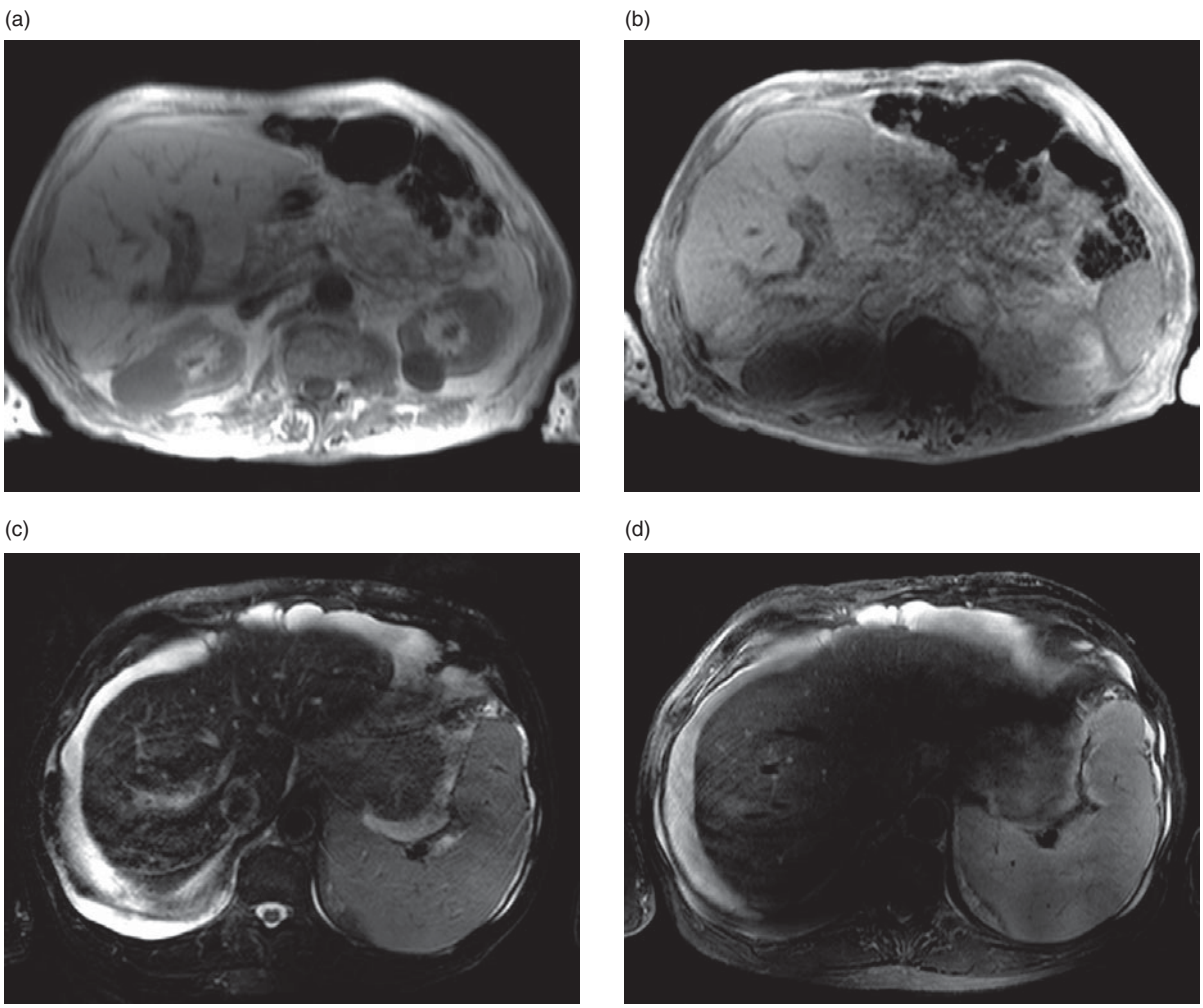

Figure 1.10 Standing wave artifacts. T1-weighted images at 1.5T (a) and 3T (b). Standing wave effects in the upper abdomen cause significant artifact at 3T. Note inhomogeneity around the spine in (b). T2-weighted images in a patient with ascites at 1.5T (c) and 3T (d). Note large region of signal dropout in the central abdomen at 3T accentuated by ascites in (d). Parameters: (a) 1.5T T1 gradient echo in-phase 200/4.4/90°, (b) 3T T1 GRE in-phase 263/2.3/75°, (c) 1.5T T2 FSE 4000/103, (d) 3T T2 FSE 2053/100.

There are many ways to attempt to alleviate the issues related to standing wave artifacts and B1 field inhomogeneity. One of the simplest ways to decrease dielectric shading is through the use of dielectric pads or "RF cushions," pads or bags of conductive fluid or gel which are placed on the region of interest in an attempt to change the shape of the torso or partially mitigate standing waves within the torso [23]. Many recent hardware advances have also resulted in significant improvements in B1 field homogeneity through more efficient and homogeneously designed RF coils as well as the use of multi-transmitter coils "tuned" to fit the body part to be imaged [24]. Combined transmit–receive coils are also in development to improve RF transmission and signal detection efficiency at 3T. These alternative coil designs are of particular importance as well, given the specific absorption rate (SAR) intensity of pulse sequences at 3T.

Specific absorption rate

The US Food and Drug Administration and the International Electrotechnical Commission limit the SAR to 4 W/kg over 15 minutes or 8 W/kg over 5 minutes, a limit intended to prevent tissues from heating more

than 1 °C. This limit holds regardless of the field strength of a magnet. When compared with 1.5T, a doubling of field strength to 3T is accompanied by a quadrupling of the SAR. At 3T, SAR limits become a much more realistic limitation to the use of pulse sequences such as fast spin echo, 3D gradient echo, and steady-state free precession sequences. As SAR also directly relates to the imaged volume, SAR limitations become more of an issue with body MR imaging than with the imaging of smaller body parts.

$$SAR \propto B_0^2 \alpha^2 DV$$

The relationship of SAR to various imaging parameters can be illustrated with the above equation where **B0** represents the magnetic field strength, **α** represents the flip angle, **D** represents the duty cycle (the number and spacing of RF pulses), and **V** represents the volume imaged. While doubling B0 quadruples SAR, altering the other parameters can mitigate these effects to avoid exceeding SAR restrictions. Decreasing flip angles can lead to significant decreases in SAR at the potential expense of prolonged acquisition time and decreased T1 contrast. More sophisticated techniques for varying flip angles include the use of RF refocusing pulse sequences such as flip angle sweep and hyperechoes at a slight cost of SNR [25, 26]. Techniques related to reducing the duty cycle of a pulse sequence include increasing TR (at the expense of prolonging scan time), decreasing the number of phase-encode or slice-select steps (at the cost of decreased spatial resolution, slice thickness, or field of view), alternating high and low SAR pulse sequences during the course of an examination, and using parallel imaging (at a slight cost of SNR – an effect which is less noticeable at 3T than at 1.5T). Imaging volume is less easily varied but can be affected by the use of more RF efficient transmit–receive coils or with the use of a shorter magnet bore.

Safety

Safety considerations remain a significant consideration when moving to a higher magnetic field strength. Implanted medical devices that are deemed MR compatible at 1.5T or lower are not necessarily approved for MR imaging at 3T. Metallic devices require further testing in the 3T environment prior to 3T approval as there is a proportional increase in translational attraction and torque upon these implanted devices with an increase in magnetic field strength [27]. This is especially true in the latest generation of wider- and shorter-bore magnets due to their increased spatial gradients and higher associated deflection angles [28]. With an ever-expanding clinical experience with 3T MR imaging, more devices will eventually gain 3T approval.

In addition to device safety, MR imaging siting issues are also important to consider with a higher field strength. A higher field strength results in a larger magnetic fringe field. This requires either a wider 5 Gauss safety margin increasing the 3T MR suite's "footprint" or the use of active shielding to counteract the larger fringe field (not without additional installation and maintenance cost). Acoustic noise concerns are also an issue with higher field strength imaging although this has been mitigated on newer scanners with improved acoustic shielding.

Conclusion

MR imaging at 3T is becoming more popular, more widespread, and increasingly accepted as the current "cutting edge" in clinical MR imaging. This is especially the case for neurologic and musculoskeletal imaging. However, the adoption of 3T in body imaging has been comparatively slower and much of this is related to the imaging challenges that a higher field strength presents in the abdomen and pelvis.

There are many differences in the behavior of protons at 3T compared with lower field strengths and this accounts for many of the artifacts encountered at 3T MR imaging. T1 relaxation times are longer with a significant effect on soft tissue contrast, particularly on pre-contrast imaging. T2* effects are more pronounced with an increase in magnetic susceptibility artifacts as well as difficulties in maintaining a homogeneous B0 field. Chemical shift artifacts of both the first and second kind are also predictably different at 3T and require adjustments in imaging parameters and changes in pulse sequence timing. And last, but definitely not least, standing wave artifacts ("dielectric shading") are a source of significant local variation in signal intensity across the larger imaging field of view utilized in the abdomen and pelvis. Many options exist in addressing these artifacts at 3T including changes in TE, use of parallel imaging, changes in bandwidth, as well as more hardware-oriented solutions such as the use of dielectric pads and various strategies employed to generate a

more homogeneous B0 and B1 field. Only when pulse sequences and image quality can be sufficiently optimized for 3T imaging can the promise of an increased SNR truly yield perceptible improvements in spatial and temporal resolution.

Acknowledgements

Special thanks to David A. Bluemke, MD, PhD and Katarzyna J. Macura, MD, PhD for their additional help and guidance during the preparation of this topic.

References

1. Vargas MI, Delavelle J, Kohler R, Becker CD, Lovblad K. Brain and spine MRI artifacts at 3 Tesla. *J Neuroradiol* 2009; **36**(2): 74–81.
2. de Bazelaire CM, Duhamel GD, Rofsky NM, Alsop DC. MR imaging relaxation times of abdominal and pelvic tissues measured in vivo at 3T: preliminary results. *Radiology* 2004; **230**(3): 652–9.
3. Bushberg J. *The Essential Physics of Medical Imaging*, 2nd edn. Philadelphia, PA, Lippincott Williams & Wilkins, 2002. pp. xvi, 933.
4. Lee JH, Garwood M, Menon R, *et al.* High contrast and fast three-dimensional magnetic resonance imaging at high fields. *Magn Reson Med* 1995; **34**(3): 308–12.
5. Wolff SD, Eng J, Balaban RS. Magnetization transfer contrast: method for improving contrast in gradient-recalled-echo images. *Radiology* 1991; **179**(1): 133–7.
6. Elster AD. How much contrast is enough? Dependence of enhancement on field strength and MR pulse sequence. *Eur Radiol* 1997; **7** Suppl 5: 276–80.
7. Fukatsu H. 3T MR for clinical use: update. *Magn Reson Med Sci* 2003; **2**(1): 37–45.
8. Krautmacher C, Willinek WA, Tschampa HJ, *et al.* Brain tumors: full- and half-dose contrast-enhanced MR imaging at 3T compared with 1.5T – initial experience. *Radiology* 2005; **237**(3): 1014–19.
9. Lewin JS, Duerk JL, Jain VR, *et al.* Needle localization in MR-guided biopsy and aspiration: effects of field strength, sequence design, and magnetic field orientation. *AJR Am J Roentgenol* 1996; **166**(6): 1337–45.
10. Olsrud J, Latt J, Brockstedt S, Romner B, Bjorkman-Burtscher IM. Magnetic resonance imaging artifacts caused by aneurysm clips and shunt valves: dependence on field strength (1.5 and 3T) and imaging parameters. *J Magn Reson Imaging* 2005; **22**(3): 433–7.
11. Chang JM, Lee JM, Lee MW, *et al.* Superparamagnetic iron oxide-enhanced liver magnetic resonance imaging: comparison of 1.5T and 3T imaging for detection of focal malignant liver lesions. *Invest Radiol* 2006; **41**(2): 168–74.
12. Simon GH, Bauer J, Saborovski O, *et al.* T1 and T2 relaxivity of intracellular and extracellular USPIO at 1.5T and 3T clinical MR scanning. *Eur Radiol* 2006; **16**(3): 738–45.
13. Li LP, Vu AT, Li BS, Dunkle E, Prasad PV. Evaluation of intrarenal oxygenation by BOLD MRI at 3T. *J Magn Reson Imaging* 2004; **20**(5): 901–4.
14. Kuhl CK, Textor J, Gieseke J, *et al.* Acute and subacute ischemic stroke at high-field-strength (3.0-T) diffusion-weighted MR imaging: intraindividual comparative study. *Radiology* 2005; **234**(2): 509–16.
15. Kuhl CK, Gieseke J, von Falkenhausen M, *et al.* Sensitivity encoding for diffusion-weighted MR imaging at 3T: intraindividual comparative study. *Radiology* 2005; **234**(2): 517–26.
16. Gruetter R, Weisdorf SA, Rajanayagan V, *et al.* Resolution improvements in in vivo 1H NMR spectra with increased magnetic field strength. *J Magn Reson* 1998; **135**(1): 260–4.
17. Katz-Brull R, Rofsky NM, Lenkinski RE. Breathhold abdominal and thoracic proton MR spectroscopy at 3T. *Magn Reson Med* 2003; **50**(3): 461–7.
18. Wehrli FW, Perkins TG, Shimakawa A, Roberts F. Chemical shift-induced amplitude modulations in images obtained with gradient refocusing. *Magn Reson Imaging* 1987; **5**(2): 157–8.
19. Cornfeld DM, Israel G, McCarthy SM, Weinreb JC. Pelvic imaging using a T1W fat-suppressed three-dimensional dual echo Dixon technique at 3T. *J Magn Reson Imaging* 2008; **28**(1): 121–7.
20. Collins CM, Liu W, Schreiber W, Yang QX, Smith MB. Central brightening due to constructive interference with, without, and despite dielectric resonance. *J Magn Reson Imaging* 2005; **21**(2): 192–6.
21. Hussain S. *Body MR Imaging: Current Practice and Future Horizons*. Scientific Assembly and Annual Meeting of Radiological Society of North America, Chicago, IL, 2006.
22. Merkle EM, Dale BM, Paulson EK. Abdominal MR imaging at 3T. *Magn Reson Imaging Clin N Am* 2006; **14**(1): 17–26.
23. Franklin KM, Dale BM, Merkle EM. Improvement in B1-inhomogeneity artifacts in the abdomen at 3T MR imaging using a radiofrequency cushion. *J Magn Reson Imaging* 2008; **27**(6): 1443–7.
24. Tomanek B, Ryner L, Hoult DI, Kozlowski P, Saunders JK. Dual surface coil with high-B1 homogeneity for